ACS EARTH AND SPACE CHEMISTRY

http://pubs.acs.org/journal/aesccq

Article

Organosulfate Formation in Proxies for Aged Sea Spray Aerosol: Reactive Uptake of Isoprene Epoxydiols to Acidic Sodium Sulfate

Madeline E. Cooke, N. Cazimir Armstrong, Ziying Lei, Yuzhi Chen, Cara M. Waters, Yue Zhang, Nicolas A. Buchenau, Monica Q. Dibley, Isabel R. Ledsky, Tessa Szalkowski, Jamy Y. Lee, Karsten Baumann, Zhenfa Zhang, William Vizuete, Avram Gold, Jason D. Surratt,* and Andrew P. Ault*

Cite This: https://doi.org/10.1021/acsearthspacechem.2c00156

Read Online

ACCESS | Metrics & More | Article Recommendations | Supporting Information

ABSTRACT: Oxidation of isoprene, the biogenic volatile organic compound (BVOC) with the highest emissions globally, is a large source of secondary organic aerosol (SOA) in the atmosphere. Particulate organosulfates formed from acid-driven reactions of the oxidation products isoprene epoxydiol (IEPOX) isomers are important contributors to SOA mass. Most studies have focused on organosulfate formation on ammonium sulfate particles, often at low pH. However, recent work has shown that sea spray aerosol (SSA) in the accumulation mode (~100 nm) is quite acidic (pH ~2) and undergoes further heterogeneous reactions with H_2SO_4 to form Na_2SO_4. Herein, we demonstrate that substantial SOA, including organosulfates, are formed on acidic sodium sulfate particles (pH = 1.4 ± 0.1) via controlled laboratory experiments. Comparable organosulfate formation was observed for acidic sodium and ammonium sulfate particles even though acidic particles with sodium versus ammonium as the primary cation formed less SOA volume. Both exhibited core-shell morphology after the reactive uptake of IEPOX; however, organosulfates were identified with Raman microspectroscopy in the core and shell of ammonium sulfate SOA particles, but only in the core for sodium sulfate SOA. Key organosulfates were also identified in ambient samples from the Galápagos Island. Our results suggest that isoprene-derived SOA formed on aged SSA is potentially an important, but underappreciated, source of SOA and organosulfates in marine and coastal regions that could modify SOA budgets.

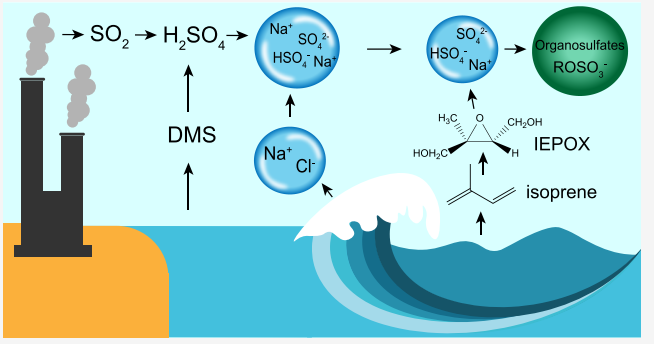

KEYWORDS: *marine secondary organic aerosol, heterogeneous chemistry, aerosol acidity, coastal aerosol chemistry, mass spectrometry, Raman microspectroscopy*

INTRODUCTION

Marine aerosol is the largest contributor to global aerosol budgets[1] and impacts Earth's radiative balance through both direct and indirect effects.[2] Understanding marine aerosol is important in both remote and coastal regions, where roughly 50% of the global population lives and where marine aerosol is an important contributor to particulate matter (PM) concentrations,[3] particularly for sub-micrometer particles.[4,5] This makes it critical to understand both primary aerosol emissions, such as sea spray aerosol (SSA),[2] and secondary aerosol that forms from oxidation of gaseous species in coastal and remote marine environments. Marine secondary aerosol includes inorganic sulfate from both natural sources (dimethyl sulfide, DMS, to SO_2 oxidation) and anthropogenic sources (ships and SO_2 emissions),[6,7] as well as organic species produced from the reactive uptake or condensation of biogenic volatile organic compound (BVOC)-derived oxidation products.[8]

Marine biota are well-established sources of isoprene,[9−11] with annual global oceanic fluxes of isoprene estimated to range from 1 to 12 Tg,[12] compared to an annual estimated total global flux of ~600 Tg.[13] Isoprene-derived secondary organic aerosol (iSOA) is known to be an important contributor to total secondary organic aerosol (SOA) in urban and continental regions,[14−16] accounting for up to 41% of the organic mass fraction in the southeast United States during summer,[17] but its formation in coastal and remote marine regions is far less understood. A major oxidation pathway for isoprene leads to the formation of isomers of isoprene epoxydiols (IEPOX).[18] IEPOX readily undergoes acid-driven reactive uptake onto ammonium sulfate (AS) particles, forming organosulfate compounds,[19] with this

Received: May 23, 2022
Revised: November 8, 2022
Accepted: November 9, 2022

reaction pathway representing up to ~30% of the particulate organosulfate mass in the eastern United States.[20] Organosulfate compounds have been identified in the atmosphere globally,[14] including in both marine[5,21,22] and continental[23,24] environments. However, most research on iSOA formation has focused on urban and continental environments,[20] while iSOA and organosulfate formation in marine environments remains much less understood.

Studies on the formation of iSOA have primarily focused on the reactive uptake of IEPOX onto ammonium sulfate salts,[19,23,25−28] which are often acidified to replicate urban aerosol pH.[29] In contrast, for marine environments, sodium is the dominant cation,[30] and sodium sulfate (SS) has long been observed to form by the reactive uptake of H_2SO_4[31−34] and displacement of HCl in numerous field studies,[7,35−37] including non-coastal cities (Atlanta)[38] and forested sites[39] hundreds of km inland (eq 1).

$$2NaCl_{(aq)} + H_2SO_{4\,(g)} \rightarrow 2HCl_{(g)} + Na_2SO_{4\,(aq)} \quad (1)$$

Recent measurements by Angle et al.[40] indicate that submicrometer marine aerosol particles are emitted with a pH of ~2. H_2SO_4 uptake can decrease the pH of SSA particles, as shown in ambient measurements by Keene et al.[41] While Nguyen et al.[42] showed that neutral SS particles do not react with IEPOX to form SOA, to our knowledge, there have not been studies that investigated the SOA production from IEPOX uptake to acidic SS particles and subsequent organosulfate formation. Research on the formation of iSOA from the reactive uptake of IEPOX onto magnesium sulfate seed particles resulted in the enhanced formation of unsaturated oligomeric species,[43] indicating that the seed impacted the chemical composition of the resultant iSOA particles.

In this study, we investigate the potential for proxies of aged SSA (Na_2SO_4 acidified with H_2SO_4) to form iSOA. iSOA was generated on acidic sodium sulfate particles reacted with gaseous *trans*-β-IEPOX, a predominant IEPOX isomer.[44] The physical and chemical transformations of the SS aerosol particles were characterized with a wide range of analytical instrumentation, including both online and offline measurements. The analytical techniques consist of a single-particle mass spectrometer (aerosol time-of-flight mass spectrometer, ATOFMS), an aerosol chemical speciation monitor (ACSM), a scanning electrical mobility spectrometer (SEMS), a Raman microspectrometer, and a particle-into-liquid sampler (PILS) whose samples were analyzed by both ion chromatography (IC) and hydrophilic interaction liquid chromatography interfaced with electrospray ionization high resolution quadrupole time-of-flight mass spectrometry (HILIC/ESI-HR-QTOFMS). We demonstrate that acidified SS seed particles are capable of forming significant amounts of iSOA and show that SS seed particles convert similar amounts of inorganic sulfates to organosulfates compared to AS-seeded iSOA particles. Furthermore, we show that SS-seeded iSOA particles result in comparable formation of methyltetrol sulfates (MTSs), which are the single most abundant organosulfates detected in ambient aerosols.[20,45,46] These results indicate that SSA, after conversion of NaCl to Na_2SO_4, could potentially be a significant source of iSOA formation in marine environments.

MATERIALS AND METHODS

Aerosol Generation. SOA was generated from the reactive uptake of *trans*-β-IEPOX, which was synthesized via the method described by Zhang et al.[47] The use of the University of North Carolina at Chapel Hill (UNC) 10 m^3 indoor chamber facility to study SOA has been described previously[48] and was operated at 50% relative humidity (RH) under dark conditions, as described by Zhang et al.[27] In short, aerosol particles were generated from solutions of SS (Sigma-Aldrich, ≥99% purity) or AS (Sigma-Aldrich, ≥99% purity) and 18.3 MΩ Milli-Q water (Table S1). The solutions were acidified by adding sulfuric acid (Sigma-Aldrich, ≥98% purity) and measured with a pH probe (Hanna Instruments). Although it has been previously shown that the aerosol pH is lower than its corresponding atomizing solution pH, the aerosol used in the present study approached the lower limit of detection for direct measurement with pH paper.[49] Thus, only the pH of the atomized solutions are reported here (Table S1). To improve run-to-run comparability, the total inorganic sulfate ($Sulf_{inorg}$), including both SO_4^{2-} and HSO_4^-, in the seed aerosol was held constant at 0.12 M, based on prior work.[50] Acidified seed particles were generated from a custom-made atomizer[28] and injected into the chamber. After the seed aerosol concentration had stabilized, gaseous *trans*-β-IEPOX was introduced to the chamber through a heated manifold (~60 °C) and injected for 60 min.

Online Analysis of Aerosol Size and Composition. A suite of analytical instruments were connected to the environmental chamber to measure real-time SOA formation, including an ATOFMS,[51] an ACSM (Q-ACSM, Aerodyne Research Inc.),[52] and a SEMS system (BMI Inc., Model 2100).[43]

Aerosol Time-of-Flight Mass Spectrometry. ATOFMS was used to measure the size and chemical composition of individual particles, and the version of ATOFMS used in this study was previously described by Pratt et al.[51] In short, aerosol particles were introduced into a differentially pumped vacuum chamber and focused into a narrow particle beam by an aerodynamic lens. The particle beam first passes through two continuous wave lasers (405 and 488 nm, respectively) 6 inches apart, and the single particle speed is measured by calculating the time taken to travel between the two lasers. Vacuum aerodynamic diameter (d_{va}) is calculated by generating a calibration curve from the particle speed of polystyrene latex sphere standards of known diameters (90 nm−1.5 μm). Based on their speed, particles are then desorbed and ionized via a Q-switched Nd:YAG laser (266 nm, fourth harmonic of a 1064 nm source), producing both positive and negative ions that are detected simultaneously via separate time-of-flight mass analyzers, providing size and dual-polarity time-of-flight mass spectra for individual particles.

Aerosol Chemical Speciation Monitor. The ACSM measures the time-resolved chemical composition of non-refractory sub-micrometer aerosol. As described in Ng et al.,[53] aerosol particles are focused into a narrow beam via an aerodynamic lens and impacted onto a hot vaporizer. The resulting vapor is ionized via electron ionization (70 eV) and analyzed via a quadrupole mass spectrometer operated in positive ion mode. ACSM calibration and tuning procedures were adopted from our prior studies.[52,54]

Scanning Electrical Mobility Sizer. The SEMS consists of a differential mobility analyzer (DMA, BMI model 2002)

https://doi.org/10.1021/acsearthspacechem.2c00156
ACS Earth Space Chem. XXXX, XXX, XXX−XXX

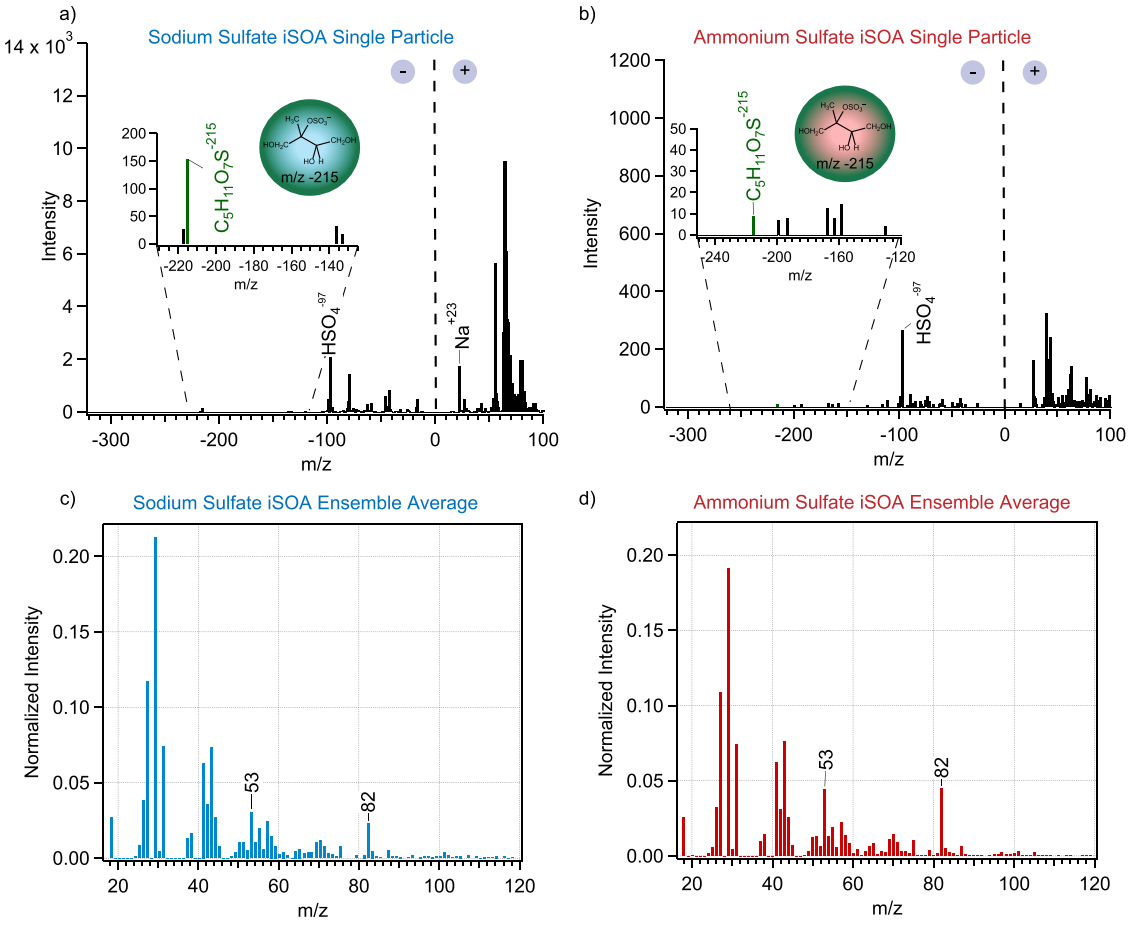

Figure 1. Single-particle mass spectra collected using the ATOFMS of SS (a) and AS (b) particles after reaction with IEPOX in an atmospheric chamber experiment. Green peak represents the monoisotopic mass of IEPOX-derived methyltetrol sulfates (an abundant organosulfate). Inset represents a zoom-in of the mass spectral region with iSOA products. ACSM organic spectra averaged for 20 min post IEPOX injection with SS (c) and AS (d) seed particles. Peaks labeled represent relevant organosulfate species. Spectra were normalized by the sum of organic species m/z 18−120.

coupled to a mixing condensation particle counter (MCPC, BMI model 1710). The SEMS measures aerosol number, surface area, and volume concentrations within the chamber at a time resolution of ∼1 min.

Offline Analysis. Laboratory Particle Collection. Particles were impacted onto quartz substrates (Ted Pella Inc.) using a multi-orifice particle sizer (MPS-3, California Measurements Inc.). Particles collected on stages 2 (0.4−2.5 μm) and 3 (<0.4 μm) were the focus of our analysis as they are closest to the peak of the particle number size distribution from the atmospheric chamber.[55] Additionally, SOA were collected by a PILS system (BMI model 4001) for offline inorganic sulfate quantification via IC, as described previously (Experiments 1 and 2;[56,57] Experiments 3 and 4[58]), and organosulfate quantification via hydrophilic interaction liquid chromatography coupled with electrospray ionization high-resolution quadrupole time of flight mass spectrometry (HILIC/ESI-HR-QTOFMS), as described previously by Cui et al.[59] The PILS vials were stored in the dark at 2 °C immediately after collection and analyzed without further pretreatment except for dilution by acetonitrile for the HILIC/ESI-HR-QTOFMS method described below.

Field Aerosol Collection and Filter Analysis. Ambient samples were collected from the Galápagos Science Center on San Cristobal Island in Puerto Baquerizo Moreno, Ecuador (0.8957°S, 89.6086°W, 15 masl), with a high-volume $PM_{2.5}$ air sampler (TE-6070 V-BL, Tisch Environmental) onto prebaked quartz filters. Sampling and extraction conditions were as described previously in Cui et al.[58] The chemical composition of the extracts were analyzed by HILIC/ESI-HR-QTOFMS as described below.

Raman Microspectroscopy. Individual particles collected onto quartz substrates during the laboratory studies were analyzed via Raman microspectroscopy with a Horiba LabRAM HR Evolution Raman Spectrometer (Horiba Scientific) coupled to a confocal optical microscope (Olympus, 100 × 0.9 N.A. objective) at ambient temperature and RH. The instrument is equipped with a ND:YAG laser source (50 mW, 532 nm) and a CCD detector. Spectra for each particle were collected in the range of 500−4000 cm^{-1} for three accumulations of 15 s. An 600 groove/mm diffraction grating with a spectral resolution of ∼1.7 cm^{-1} was used.

Ion Chromatography. IC was used to quantify the inorganic sulfate concentration in the SOA particles from the chamber. For Experiments 1 and 2, a 500 μL aliquot was analyzed by an anion exchange IC (Dionex ICS-2100) equipped with a guard column (Dionex IonPac AG18, 4 mm × 50 mm) and an anion exchange column (4 mm × 250 mm, Thermo Fisher) run at a flow rate of 1.0 L min^{-1}. For Experiments 3 and 4, a 25 μL aliquot of each PILS aqueous

https://doi.org/10.1021/acsearthspacechem.2c00156
ACS Earth Space Chem. XXXX, XXX, XXX−XXX

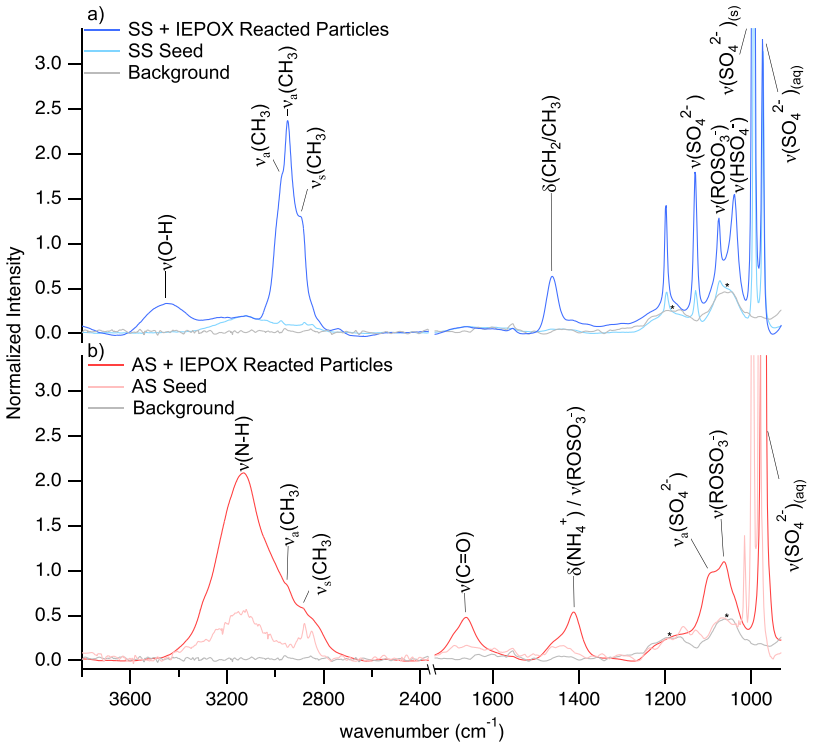

Figure 2. Raman spectra of SS (a) and AS (b) seed particles compared to the spectra of seed particles after reaction with IEPOX. For SS + IEPOX, 98 particles were analyzed and averaged; for the well-characterized AS + IEPOX, 82 particles were analyzed and averaged. Intensity for all spectra is normalized to 792 cm^{-1}, an intense peak associated with the quartz substrate. Asterisks correspond to other peaks associated with quartz substrate.

sample was analyzed by an anion exchange IC (ICS 3000, ThermoFisher). The instrument is equipped with an IonPac AS11-HC guard column (2 mm × 50 mm ThermoFisher) and an anion-exchange column (2 mm × 250 mm ThermoFisher) run at a flow rate of 0.4 L min^{-1}.

Hydrophilic Interaction Liquid Chromatography Interfaced with Electrospray Ionization High-Resolution Quadrupole Time-of-Flight Mass Spectrometry. HILIC/ESI-HR-QTOFMS was used to quantify the concentration of methyltetrol sulfates (MTSs) in the iSOA particles, the predominant IEPOX-derived organosulfate compounds,[45,58,60,61] and 2-methyltetrols (2-MTs) from the laboratory and field. As previously described by Chen et al.,[58] a 50 μL aliquot of each PILS aqueous sample was withdrawn and diluted in 950 μL of acetonitrile (ACN, HPLC-grade, Fisher Scientific) shortly after collection in order to achieve the solvent composition of the organic mobile phase (i.e., 95:5 ACN:H_2O). Diluted PILS samples were stored in the dark at −20 °C prior to HILIC/ESI-HR-QTOFMS analysis. Analysis was performed following the method of Chen et al.[58] using an Agilent 6520 Series Accurate Mass Q-TOFMS with an ESI source operated in negative mode coupled to an Agilent 6500 Series UPLC equipped with a Waters ACQUITY UPLC BEH Amide column following the published method.[58] The operating conditions of the HILIC/ESI-QTOFMS system (elution gradient program, mass calibration, tuning, voltages, etc.) were previously described by Chen et al.[58]

RESULTS AND DISCUSSION

Identification of Organosulfate Formation. Atmospheric chamber experiments were conducted with both acidified SS (pH 1.4 ± 0.1) and acidified AS (pH 1.4 ± 0.1) seed particles and reacted with IEPOX. The chemical composition of the reacted particles was monitored at the single-particle level with ATOFMS and at the bulk aerosol level with an ACSM. IEPOX-derived MTS isomers have been previously observed in ambient particles from field measurements using the ATOFMS as deprotonated molecules ($C_5H_{11}O_7S^-$) at a mass-to-charge ratio (m/z) of 215.[38,62] ATOFMS spectra from organosulfate standards including 3-methyltetrol organosulfates, sodium ethyl sulfate, and hydroxyacetone sulfate were compared (Figure S1). A negative ion peak at m/z 215 was only observed in the spectrum for 3-methyltetrol organosulfates, whereas no peak was observed at m/z 215 in the spectra for the remaining standards, providing further evidence that this peak corresponds to MTS isomers. A negative ion peak at m/z 215 was observed in the ATOFMS spectra of the reacted particles for both AS and SS seed aerosol, indicating that MTS isomers can form from the reaction of IEPOX with sulfate on the acidified SS seed particles. Example ATOFMS spectra of individual particles are shown for acidic SS + IEPOX and acidic AS + IEPOX-reacted particles (Figure 1a,b). We observed particle-to-particle variability in the collected ATOFMS spectra of SS + IEPOX reacted particles, which can be noted in the lower m/z region of the SS + IEPOX-reacted particles (Figure S2). In addition to MTS isomers observed as deprotonated molecules at m/z 215, the SS-reacted particles contained other isoprene-derived organic compounds previously identified in ambient aerosol: glycolic acid sulfates with deprotonated molecules at m/z 155 and 2-MTs with deprotonated molecules at m/z 135 (Figure S2).[62]

Bulk aerosol average mass spectra from the ACSM demonstrate that organic aerosol forms from the reaction of IEPOX with acidified SS particles (Figure 1c). The average

https://doi.org/10.1021/acsearthspacechem.2c00156
ACS Earth Space Chem. XXXX, XXX, XXX−XXX

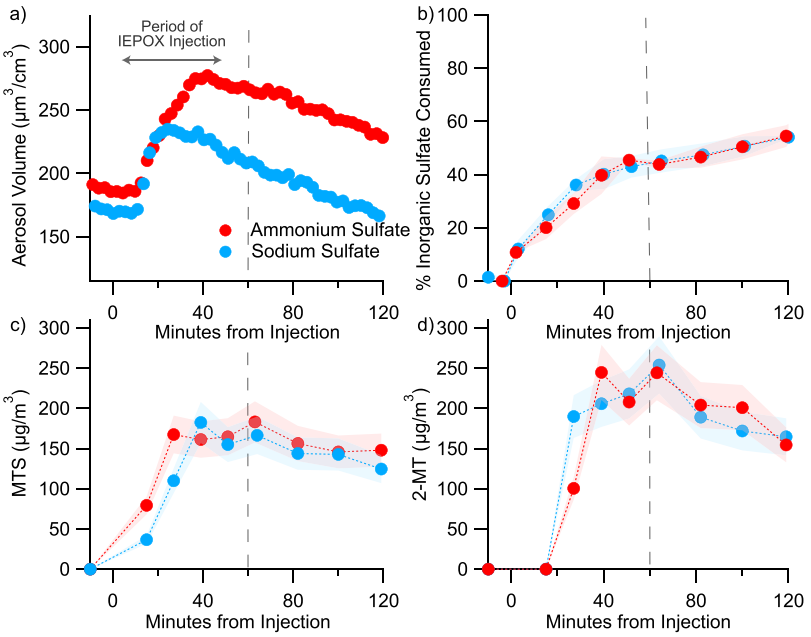

Figure 3. Change in aerosol volume, inorganic sulfate, methyltetrol sulfates (MTS), and 2-methyltetrols (2-MT) for SS (blue) and AS (red) seed particles at pH = 1.4 ± 0.1 reacted with IEPOX in an atmospheric chamber. (a) Change in aerosol volume for SS-seeded and AS-seeded iSOA particles. (b) Change in the percentage of inorganic sulfate consumed. Shaded region represents standard deviation for IC analysis. (c) Change in the mass of MTSs. Shaded region represents % relative error for HILIC/ESI-HR-QTOFMS analysis. (d) Change in the mass of 2-MTs. Shaded region represents % relative error for HILIC/ESI-HR-QTOFMS analysis.

organic ACSM mass spectra of SOA produced following 60 min of IEPOX injection were compared for the AS and SS seed particles (Figure 1c,d). The AS and SS experiments produce similar SOA spectra, with both containing mass spectral fragments at m/z 53 and 82,[48] characteristic ACSM mass fragment ions for IEPOX-derived organic compounds.[17,52] The combined ACSM and ATOFMS results support the conclusion that organic aerosol forms from the reaction of IEPOX with acidified SS aerosol via single-particle and bulk analysis.

Impact of Seed on SOA Chemical Composition and Morphology. To further differentiate inorganic and organic sulfate within individual particles, Raman spectra were collected for the SS and AS seed particles and compared to the particles after reaction with IEPOX in the atmospheric chamber (Figure 2 and Table S2). Inorganic sulfate (aqueous) is discernable and located in the seed and reacted particles for both SS and AS particles at 974 and 972 cm^{-1}, respectively, in the form of the sulfate symmetric stretching mode, $\nu_s(SO_4^{2-})$,[63] and in the SS-reacted aerosol particles at 1039 in the form of bisulfate $\nu(HSO_4^-)$.[63] For both seed aerosol types, the spectra show the formation of organic compounds observed via the methyl asymmetric stretching mode in the C−H stretching region (2950, 2974, and 2952 cm^{-1}),[64] methyl symmetric stretching mode (2897 and 2892 cm^{-1}),[64] and additional organic modes in the fingerprint region (1663, 1462, 1410, 1075, and 1063 cm^{-1}).[65−69] Peaks at 1075 and 1063 cm^{-1} in the spectra of the SS- and AS-reacted particles, respectively, correspond to IEPOX-derived organosulfates.[65,70]

The spectra also indicate chemical differences between the SS-reacted aerosol particles and AS-reacted aerosol particles. In the AS-reacted aerosol particles, we observed a peak at 1410 cm^{-1}, potentially corresponding to the ammonium bend,[69,70] though neutral organosulfate compounds or other organic modes may also contribute.[65,69,70] In the AS-seeded iSOA, we also observed a peak corresponding to carbonyls at 1663 cm^{-1}.[71] This peak was not observed in the SS particles, suggesting that different products may form in SS-seeded iSOA particles. We also observed a distinct peak in the fingerprint region for the SS particles corresponding to the CH_2/CH_3 bend at 1462 cm^{-1}.[65] Comparing the Raman spectra of the reacted to the seed particles for acidified SS further supports our conclusion that organic aerosol forms from the reaction of IEPOX with SS seed aerosol.

Impact of Seed Aerosol Type on SOA Mass and Organosulfate Formation. To investigate how the main cation (Na^+ vs NH_4^+) in the seed aerosol impacts the formation of organosulfate compounds, SEMS was used to determine aerosol volume formation, IC was used to quantify the percentage of inorganic sulfate consumed, and HILIC/ESI-HR-QTOFMS was used to quantify MTSs and 2-MTs formed in the iSOA during the atmospheric chamber experiments for SS and AS (Figure 3). After 60 min of reaction in the chamber, the volume of SOA formation was greater from the reaction of acidic AS with IEPOX than that from the reaction of acidic SS with IEPOX. Despite the difference in aerosol volume growth, the percentage of inorganic sulfate consumption at 60 min was similar for AS (44% ± 4) and SS (45% ± 4) at 60 min, indicating that a comparable amount of organosulfates is formed for both seed types. We also investigated the mass of key iSOA products MTSs and 2-MTs at 60 min. The mass of MTSs formed at 60 min from the reaction of acidic AS with IEPOX (180 ± 30 $\mu g/m^3$) was comparable to the amount formed from the reaction of acidic SS with IEPOX (170 ± 20 $\mu g/m^3$) as well as the mass of 2-MTs formed at 60 min for AS SOA (240 ± 30 $\mu g/m^3$) and SS SOA (250 ± 30 $\mu g/m^3$).

We compared the time-resolved volume, inorganic sulfate consumption, MTS mass, and 2-MT mass for SS and AS seed aerosol types (Figure 3). SEMS results indicate that AS-seeded iSOA particle volume growth is greater than iSOA formed from SS seed aerosol particles (Figure 3a). The volume growth

https://doi.org/10.1021/acsearthspacechem.2c00156
ACS Earth Space Chem. XXXX, XXX, XXX−XXX

for the SS and AS experiments were similar until ~20 min after the reaction began, when SS-seeded iSOA particles started to level off and AS-seeded iSOA particles continued to increase. For iSOA from both AS and SS seed aerosols, the amount of inorganic sulfate began decreasing at the beginning of IEPOX injection, indicating that the inorganic sulfate was consumed and converted to organosulfates immediately after reaction with gaseous IEPOX. After 60 min, the injection of IEPOX was stopped and the particles were allowed to react in the chamber for another 60 min. For both the SS- and AS-seeded iSOA particles, the inorganic sulfate continued to be consumed, indicating that further chemical reactions involving sulfate incorporation into organic species were occurring. However, the decrease occurred at a slower rate than during the period of IEPOX injection.

Similar to inorganic sulfate consumption, the formation of MTS and 2-MT products were comparable for the two seed types. The mass of MTSs increased until about 20 min into the reaction, around the same time that the volume formation leveled off in the SS-iSOA and the AS-iSOA continued to increase. After ~30 min of reaction, the MTS mass stopped increasing and remained stable for the experiment for both inorganic seed particle types. The 2-MT mass increased in both the AS and SS iSOA until ~40 min of reaction, after which the mass of 2-MTs in the iSOA slowly decreased in the particles, potentially due to wall loss, for the remainder of the experiment.

The experiments for both particle types were repeated, and a similar trend was observed with increased volume formation in the AS-seeded iSOA compared to the SS-seeded iSOA (Figure S3). The particle size distributions were compared for the SS and AS seed aerosol particles reacted with IEPOX at 0 min (unreacted), 30 min reaction, and 60 min reaction (Figure S4). For both the SS and AS experiments, the particle size modes were similar. Slightly greater MTS and 2-MT masses of formation were observed in the repeats that can be attributed to a greater mass of IEPOX injected during the AS repeat experiment (3.9 mg) compared to the SS (2.9 mg), though other factors, including partitioning and formation of other products, could play a role.

HILIC/ESI-HR-QTOFMS was used to investigate the formation of other known organosulfate products in the iSOA. Similar product formation was observed in the iSOA formed from the two particle types. Future studies will be conducted to compare the product distribution in iSOA-formed IEPOX with acidic SS and acidic AS.

Particle Morphology. To investigate the potential for SS seed particles to form a core-shell morphology, potentially resulting in the "self-limiting" effect as described by Zhang et al.,[72] single-particle morphology and chemical composition was investigated using Raman microspectroscopy for SS- and AS-seeded iSOA particles. Both SS- and AS-derived iSOA particles formed core-shell morphologies after reacting with IEPOX (Figure 4 and Table S3), as observed by the optical image of each particle as well as the chemical differences obtained from the spectra taken at the center (core) and edge of the particle (shell). Core and shell spectra for particles (AS, n = 18; SS n = 25) were compared to assess reproducibility (Figures S5 and S6).

For SS-reacted particles, an organic peak at 1077 cm^{-1} was observed in the core, corresponding to organosulfates.[70] Inorganic sulfate was observed in the core and the shell in the form of aqueous sulfate at 997 cm^{-1},[64] solid sodium sulfate

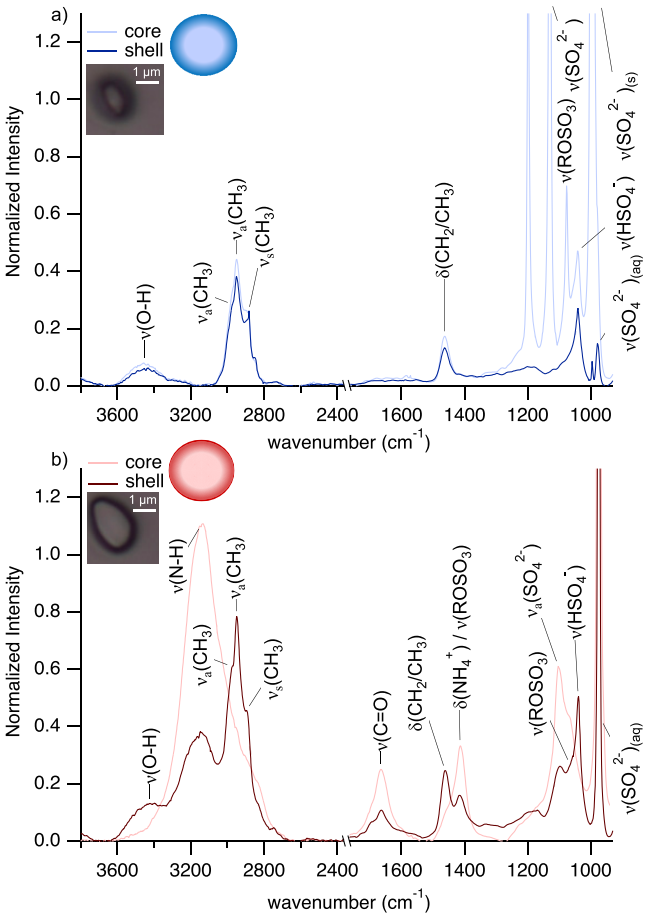

Figure 4. Representative single-particle Raman spectrum for the core and shell of (a) SS seed particles + IEPOX and (b) AS seed particles + IEPOX. Inset shows 100× optical microscope image of aerosol particle corresponding to the spectrum.

at 996 cm^{-1},[64] and bisulfate at 1042 cm^{-1} as identified by Chen et al.[63] The core and shell also contained peaks at 1462 corresponding to bending modes for CH_2/CH_3 groups and three peaks at 2885, 2951, and 2974 cm^{-1} corresponding to $\nu_s(CH_3)$,[64] $\nu_a(CH_3)$,[64] and $\nu_a(CH_3)$,[65] respectively. Interestingly, the same peak shape with $\nu_s(CH_3)$[64] (2896) and $\nu_a(CH_3)$[64,65] (2950 and 2974) was observed in the shell of the AS particles as well, indicating that the shell of the SS and AS particles likely has a similar organic composition. The shell of the SS particles did not contain a peak representative of organosulfates, indicating that the shell is likely composed of other non-sulfated organic compounds. The core and shell spectra were compared for n = 18 particles (Figure S5), and little particle-to-particle variability was noted. The peaks discussed above were observed in all of the spectra, but there was some variability in the relative intensity of the peaks. These results indicate that, like AS-seeded iSOA particles, both the core and shell of the SS-reacted particles contain organic compounds, which could result in a self-limiting effect in the reactive uptake of IEPOX onto acidic SS particles.[27]

The core and shell for AS-reacted particles were compared as well, and two particle types were observed. The first particle type resembled those previously observed by Olson et al.,[73] with a chemically distinct core and shell. The second particle type was homogeneous with no apparent differences between the core and shell. These particles had a notable absence of a

https://doi.org/10.1021/acsearthspacechem.2c00156
ACS Earth Space Chem. XXXX, XXX, XXX−XXX

peak associated with the N−H stretch, indicating that the ammonium may have partitioned out of the particles as ammonia after reaction with IEPOX. Six examples of each particle type are shown (Figure S6), and a representative particle for the core-shell morphology is provided (Figure 4).

In the AS-seeded core-shell particles, an organosulfate mode was identified in the core and shell particles at 1065 cm^{-1}, agreeing with the results from Olson et al.[73] The $\nu_a(CH_3)$ stretching modes at 2974 and 2950 cm^{-1} as well as the $\nu_s(CH_3)$ stretching mode at 2896 cm^{-1} were observed only in the shell of the AS particles, whereas the carbonyl stretch at 1666 cm^{-1} and the CH_2/CH_3 bending modes at 1461 cm^{-1} were observed in both the core and the shell. These results suggest that the AS-reacted seed particles result in the formation of iSOA particles with different morphologies than those formed from SS seed particles.

The SS- and AS-iSOA particles were reanalyzed 1 month after the experiment was conducted, and it was found that the chemical compositions of both particle types had changed (Figure S7). Ammonium was observed in the SS-iSOA, suggesting that ammonia partitioned into the iSOA particles during the 1 month of storage in the laboratory. Additionally, ammonium was present in both the core and shell of the AS-iSOA, whereas it was only observed in the core of the particles analyzed shortly after the experiment was conducted. These results indicate the potential for both SS-iSOA and AS-iSOA to undergo further reactions after formation in the atmosphere that could alter the particle morphology, as well as chemical composition.

Organosulfate Identification in an Ambient Marine Environment. To assess the potential for iSOA and organosulfates to form on SS in an ambient marine-influenced atmosphere, filter samples were collected from the Galápagos Islands of Ecuador. The aerosol composition was analyzed using the HILIC/ESI-HR-QTOFMS method. Methyltetrol sulfates were observed in the extracted ion chromatogram (EIC) for the negative ion at m/z 215.0231 (Figure 5). As

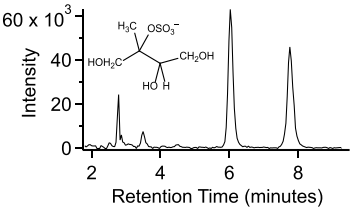

Figure 5. HILIC/ESI-HR-QTOFMS extracted ion chromatogram (EIC) for methyltetrol sulfates at m/z −215.0231 in a PM2.5 sample collected from the Galápagos Islands, Ecuador.

Galápagos Islands are a remote environment with primarily marine and, to a lesser extent, terrestrial influences, these organosulfates could be forming from the reaction of IEPOX with smaller SSA, which were recently shown to be very acidic (pH ≈ 2).[40] The same number of peaks for the MTS isomers, corresponding to the structural isomers for 2-MTS and 3-MTS as previously shown,[59] and their relative positions (2.7, 3.5, 6.0, and 7.8 min) were observed in the aerosol sample collected from the Galápagos Islands (Figure 5) as were observed in prior HILIC/ESI-HR-QTOFMS data reported by Cui et al.[59] While the formation of iSOA has been primarily investigated in continental environments, the presence of MTSs from a remote environment with marine influences demonstrates that iSOA from the reaction of IEPOX with aged SSA is an unrecognized and likely important source of MTSs.

Atmospheric Implications. SSA is the largest source of aerosol emissions to the atmosphere,[1] and freshly emitted submicron SSA were recently shown to have a pH of ∼2.[40,74] SSA particles intrinsically contain SS salts, and the amount of sulfate increases substantially after heterogeneous reactions with H_2SO_4.[35] Thus, it is important to consider the potential of these particles to seed the formation of iSOA. This study demonstrates that acidified SS particles (pH 1.4 ± 0.1) are capable of seeding the formation of iSOA, resulting in particles with similar amounts of inorganic sulfate incorporated into organosulfates and formation of similar amounts of MTSs when compared to the more-studied iSOA particles formed on AS seed aerosol. As such, SS particles in SSA should be considered when modeling iSOA formation in marine environments in order to accurately predict their formation and impact on the climate. More so, ambient measurements indicate that marine aerosol can undergo long-range atmospheric transport,[3,39,75] and thus, may be a source of iSOA in continental regions in addition to marine environments. The experiments conducted in this study isolated the initial reactive uptake of IEPOX onto particulate sulfate but did not account for additional chemical processes that could occur in ambient marine and coastal environments. Further studies should investigate the potential of SS- and AS-seeded iSOA to undergo photolysis reactions, heterogeneous reactions with other organic gases beyond IEPOX, or further aging via oxidation with OH, which could impact the chemical compositions and physical properties of these particles. Further research is needed on the potential of SSA to seed the formation of organosulfate compounds globally, particularly as a function of aerosol acidity, and their impact on climate.

■ ASSOCIATED CONTENT

Supporting Information

The Supporting Information is available free of charge at https://pubs.acs.org/doi/10.1021/acsearthspacechem.2c00156.

(Table S1) Additional information including atmospheric chamber experimental conditions; (Figure S1) single-particle mass spectra for standards: methyltetrol sulfates, sodium ethyl sulfate, and hydroxyacetone sulfate; (Figure S2) four single-particle mass spectra for SS seed particles reacted with IEPOX; (Table S2) experimentally determined Raman modes and tentative assignments for SS and AS seed particles before and after reaction with IEPOX; (Figure S3) change in aerosol volume, inorganic sulfate consumption, MTS, and 2-MT formation for additional experiments; (Figure S4) size distributions for SS- and AS-derived iSOA; (Table S3) experimentally determined Raman modes and tentative assignments for the core (center) and shell (edge) of SS and AS seed particles reacted with IEPOX; (Figure S5) core and shell Raman spectra for SS iSOA; (Figure S6) core and shell Raman spectra for AS iSOA; (Figure S7) core and shell Raman spectra for SS- and AS-derived iSOA after one month of storage (PDF)

https://doi.org/10.1021/acsearthspacechem.2c00156
ACS Earth Space Chem. XXXX, XXX, XXX−XXX

AUTHOR INFORMATION

Corresponding Authors

Andrew P. Ault − *Department of Chemistry, University of Michigan, Ann Arbor, Michigan 48109, United States;* orcid.org/0000-0002-7313-8559; Email: aulta@umich.edu

Jason D. Surratt − *Department of Environmental Sciences and Engineering, Gillings School of Global Public Health and Department of Chemistry, College of Arts and Sciences, University of North Carolina at Chapel Hill, Chapel Hill, North Carolina 27599, United States;* orcid.org/0000-0002-6833-1450; Email: surratt@unc.edu

Authors

Madeline E. Cooke − *Department of Chemistry, University of Michigan, Ann Arbor, Michigan 48109, United States*

N. Cazimir Armstrong − *Department of Environmental Sciences and Engineering, Gillings School of Global Public Health, University of North Carolina at Chapel Hill, Chapel Hill, North Carolina 27599, United States*

Ziying Lei − *Department of Environmental Health Sciences, University of Michigan, Ann Arbor, Michigan 48109, United States;* Present Address: Present address: Department of Atmospheric Sciences, Texas A&M University, College Station, Texas 77843, United States (Z.L.); orcid.org/0000-0003-3071-0698

Yuzhi Chen − *Department of Environmental Sciences and Engineering, Gillings School of Global Public Health, University of North Carolina at Chapel Hill, Chapel Hill, North Carolina 27599, United States;* orcid.org/0000-0002-2547-8428

Cara M. Waters − *Department of Chemistry, University of Michigan, Ann Arbor, Michigan 48109, United States*

Yue Zhang − *Department of Environmental Sciences and Engineering, Gillings School of Global Public Health, University of North Carolina at Chapel Hill, Chapel Hill, North Carolina 27599, United States; Aerodyne Research Inc., Billerica, Massachusetts 01821, United States;* Present Address: Present address: Department of Atmospheric Sciences, Texas A&M University, College Station, Texas 77843, United States (Z.L.); orcid.org/0000-0001-7234-9672

Nicolas A. Buchenau − *Department of Environmental Sciences and Engineering, Gillings School of Global Public Health, University of North Carolina at Chapel Hill, Chapel Hill, North Carolina 27599, United States;* Present Address: Present address: Picarro Inc., Morrisville, North Carolina 27560, United States (K.B.)

Monica Q. Dibley − *Department of Chemistry, University of Michigan, Ann Arbor, Michigan 48109, United States*

Isabel R. Ledsky − *Department of Chemistry, Carleton College, Northfield, Minnesota 55057, United States*

Tessa Szalkowski − *Department of Environmental Sciences and Engineering, Gillings School of Global Public Health, University of North Carolina at Chapel Hill, Chapel Hill, North Carolina 27599, United States*

Jamy Y. Lee − *Department of Chemistry, University of Michigan, Ann Arbor, Michigan 48109, United States;* orcid.org/0000-0002-3680-5797

Karsten Baumann − *Department of Environmental Sciences and Engineering, Gillings School of Global Public Health, University of North Carolina at Chapel Hill, Chapel Hill, North Carolina 27599, United States;* orcid.org/0000-0003-4045-5539

Zhenfa Zhang − *Department of Environmental Sciences and Engineering, Gillings School of Global Public Health, University of North Carolina at Chapel Hill, Chapel Hill, North Carolina 27599, United States*

William Vizuete − *Department of Environmental Sciences and Engineering, Gillings School of Global Public Health, University of North Carolina at Chapel Hill, Chapel Hill, North Carolina 27599, United States;* orcid.org/0000-0002-1399-2948

Avram Gold − *Department of Environmental Sciences and Engineering, Gillings School of Global Public Health, University of North Carolina at Chapel Hill, Chapel Hill, North Carolina 27599, United States;* orcid.org/0000-0003-1383-6635

Complete contact information is available at: https://pubs.acs.org/10.1021/acsearthspacechem.2c00156

Funding

This work was supported by the National Science Foundation (NSF) under grants AGS-1703019 and AGS-2040610 (A.P.A.) as well as AGS-1703535 and AGS-2039788 (J.D.S.). Y.Z acknowledges support from an NSF Postdoctoral Fellowship (AGS-1524731). A.G., Z.Z., and J.D.S. also acknowledge support from NSF grant no. AGS-2001027 (A.G.). M.E.C. was supported by an NSF Graduate Research Fellowship (NSF-GRFP) DGE-1841052.

Notes

The authors declare no competing financial interest.

ACKNOWLEDGMENTS

Prof. Barb Turpin and her research group are gratefully acknowledged for allowing us to use the PILS and IC instrumentation during the initial experiments. Prof. Kerri Pratt and her research group are also gratefully acknowledged for allowing us to use ATOFMS and for later experiment the IC instrumentation.

REFERENCES

(1) De Leeuw, G.; Andreas, E. L.; Anguelova, M. D.; Fairall, C. W.; Lewis, E. R.; O'Dowd, C.; Schulz, M.; Schwartz, S. E. Production flux of sea spray aerosol. *Rev. Geophys.* **2011**, *49*, 1−39.

(2) Quinn, P. K.; Collins, D. B.; Grassian, V. H.; Prather, K. A.; Bates, T. S. Chemistry and related properties of freshly emitted sea spray aerosol. *Chem. Rev.* **2015**, *115*, 4383−4399.

(3) Gaston, C. J.; Pratt, K. A.; Qin, X.; Prather, K. A. Real-Time Detection and Mixing State of Methanesulfonate in Single Particles at an Inland Urban Location during a Phytoplankton Bloom. *Environ. Sci. Technol.* **2010**, *44*, 1566−1572.

(4) Mayer, K. J.; Wang, X.; Santander, M. V.; Mitts, B. A.; Sauer, J. S.; Sultana, C. M.; Cappa, C. D.; Prather, K. A. Secondary Marine Aerosol Plays a Dominant Role over Primary Sea Spray Aerosol in Cloud Formation. *ACS Cent. Sci.* **2020**, *6*, 2259−2266.

(5) Cui, T.; Green, H. S.; Selleck, P. W.; Zhang, Z.; O'Brien, R. E.; Gold, A.; Keywood, M.; Kroll, J. H.; Surratt, J. D. Chemical Characterization of Isoprene- and Monoterpene-Derived Secondary Organic Aerosol Tracers in Remote Marine Aerosols over a Quarter Century. *ACS Earth Space Chem.* **2019**, *3*, 935−946.

(6) Corbett, J. J.; Fischbeck, P. S.; Pandis, S. N. Global nitrogen and sulfur inventories for oceangoing ships. *J. Geophys. Res.: Atmos.* **1999**, *104*, 3457−3470.

(7) Ault, A. P.; Moore, M. J.; Furutani, H.; Prather, K. A. Impact of Emissions from the Los Angeles Port Region on San Diego Air

Quality during Regional Transport Events. *Environ. Sci. Technol.* **2009**, *43*, 3500−3506.
(8) Hallquist, M.; Wenger, J. C.; Baltensperger, U.; Rudich, Y.; Simpson, D.; Claeys, M.; Dommen, J.; Donahue, N. M.; George, C.; Goldstein, A. H.; Hamilton, J. F.; Herrmann, H.; Hoffmann, T.; Iunuma, Y.; Jang, M.; Jenkin, M. E.; Jimenez, J. L.; Kiendler-Scharr, A.; Maenhaut, W.; McFiggans, G.; Mentel, T. F.; Monod, A.; Prevot, A. S. H.; Seinfeld, J. H.; Surratt, J. D.; Szmigielski, R.; Wildt, J. The formation, properties and impact of secondary organic aerosol: current and emerging issues. *Atmos. Chem. Phys.* **2009**, *9*, 5155−5236.
(9) Bonsang, B. P.; Lambert, G. Evidence for marine production of isoprene. *Geophys. Res. Lett.* **1992**, *19*, 1129−1132.
(10) Shaw, S. L.; Gantt, B.; Meskhidze, N. Production and Emissions of Marine Isoprene and Monoterpenes: A Review. *Adv. Meteor.* **2010**, *2010*, 1−24.
(11) Ciuraru, R.; Fine, L.; Pinxteren, M. V.; D'Anna, B.; Herrmann, H.; George, C. Unravelling New Processes at Interfaces: Photochemical Isoprene Production at the Sea Surface. *Environ. Sci. Technol.* **2015**, *49*, 13199−13205.
(12) Luo, G. A numerical evaluation of global oceanic emissions of a-pinene and isoprene. *Atmos. Chem. Phys.* **2010**, *10*, 2007−2015.
(13) Guenther, A.; Karl, T.; Harley, P.; Wiedinmyer, C.; Palmer, P. I.; Geron, C. Estimates of global terrestrial isoprene emissions using MEGAN (Model of Emissions of Gases and Aerosols from Nature). *Atmos. Chem. Phys.* **2006**, *6*, 3181−3210.
(14) Bruggemann, M.; Xu, R.; Tilgner, A.; Kwong, K. C.; Mutzel, A.; Poon, H. Y.; Otto, T.; Schaefer, T.; Poulain, L.; Chan, M. N.; Herrmann, H. Organosulfates in Ambient Aerosol: State of Knowledge and Future Research Directions on Formation, Abundance, Fate, and Importance. *Environ. Sci. Technol.* **2020**, *54*, 3767−3782.
(15) Turpin, B. J. Identification of Secondary Organic Aerosol Episodes and Quantitation of Primary and Secondary Organic Aerosol Concentrations During SCAQS. *Atmos. Environ.* **1995**, *29*, 3527−3544.
(16) Carlton, A.; Kroll, J. H. A review of Secondary Organic Aerosol (SOA) formation from isoprene. *Atmos. Chem. Phys.* **2009**, *9*, 4987−5005.
(17) Budisulistiorini, S. H.; Baumann, K.; Edgerton, E. S.; Bairai, S. T.; Mueller, S.; Shaw, S. L.; Knipping, E. M.; Gold, A.; Surratt, J. D. Seasonal characterization of submicron aerosol chemical composition and organic aerosol sources in the southeastern United States: Atlanta, Georgia,and Look Rock, Tennessee. *Atmos. Chem. Phys.* **2016**, *16*, 5171−5189.
(18) Paulot, F.; Crounse, J. D.; Kjaergaard, H. G.; Kurten, A.; St. Clair, J. M.; Seinfeld, J. H.; Wennberg, P. O. Unexpected Epoxide Formation in the Gas-Phase Photooxidation of Isoprene. *Science* **2009**, *325*, 730−733.
(19) Surratt, J. D. G.-G.; Chan, A. W. H.; Vermeylen, R.; Shahgholi, M.; Kleindienst, T. E.; Edney, E. O.; Offenberg, J. H.; Lewandowski, M.; Jaoui, M.; Maenhaut, W.; Claeys, M.; Flagan, R. C.; Seinfeld, J. H. Organosulfate Formation in Biogenic Secondary Organic Aerosol. *J. Phys. Chem. A* **2008**, *112*, 8345−8378.
(20) Chen, Y.; Dombek, T.; Hand, J.; Zhang, Z.; Gold, A.; Ault, A. P.; Levine, K. E.; Surratt, J. D. Seasonal Contribution of Isoprene-Derived Organosulfates to Total Water-Soluble Fine Particulate Organic Sulfur in the United States. *ACS Earth Space Chem.* **2021**, *5*, 2419−2432.
(21) Stone, E. A.; Yang, L.; Yu, L. E.; Rupakheti, M. Characterization of organosulfates in atmospheric aerosols at Four Asian locations. *Atmos. Environ.* **2012**, *47*, 323−329.
(22) Hawkins, L. N.; Russell, L. M.; Covert, D. S.; Quinn, P. K.; Bates, T. S.Carboxylic acids, sulfates, and organosulfates in processed continental organic aerosol over the southeast Pacific Ocean during VOCALS-REx 2008. *J. Geophys. Res.: Atmos.***2010**, *115* (), DOI: 10.1029/2009JD013276.
(23) Surratt, J. D. K.; Kleindienst, T. E.; Edney, E. O.; Claeys, M.; Sorooshian, A.; Ng, N. L.; Offenberg, J. H.; Lewandowski, M.; Jaoui, M.; Flagan, R. C.; Seinfeld, J. H. Evidence for organosulfates in secondary organic aerosol. *Environ. Sci. Technol.* **2007**, *41*, 517−527.
(24) Kristensen, K.; Glasius, M. Organosulfates and oxidation products from biogenic hydrocarbons in fine aerosols from a forest in North West Europe during spring. *Atmos. Environ.* **2011**, *45*, 4546−4556.
(25) Gaston, C. J.; Riedel, T. P.; Zhang, Z.; Gold, A.; Surratt, J. D.; Thornton, J. A. Reactive uptake of an isoprene-derived epoxydiol to submicron aerosol particles. *Environ. Sci. Technol.* **2014**, *48*, 11178−11186.
(26) Surratt, J. D.; Chan, A. W.; Eddingsaas, N. C.; Chan, M.; Loza, C. L.; Kwan, A. J.; Hersey, S. P.; Flagan, R. C.; Wennberg, P. O.; Seinfeld, J. H. Reactive intermediates revealed in secondary organic aerosol formation from isoprene. *Proc. Natl. Acad. Sci. U. S. A.* **2010**, *107*, 6640−6645.
(27) Zhang, Y.; Chen, Y.; Lei, Z.; Olson, N. E.; Riva, M.; Koss, A. R.; Zhang, Z.; Gold, A.; Jayne, J. T.; Worsnop, D. R.; Onasch, T. B.; Kroll, J. H.; Turpin, B. J.; Ault, A. P.; Surratt, J. D. Joint Impacts of Acidity and Viscosity on the Formation of Secondary Organic Aerosol from Isoprene Epoxydiols (IEPOX) in Phase Separated Particles. *ACS Earth Space Chem.* **2019**, *3*, 2646−2658.
(28) Riva, M.; Chen, Y.; Zhang, Y.; Lei, Z.; Olson, N. E.; Boyer, H. C.; Narayan, S.; Yee, L. D.; Green, H. S.; Cui, T.; Zhang, Z.; Baumann, K.; Fort, M.; Edgerton, E.; Budisulistiorini, S. H.; Rose, C. A.; Ribeiro, I. O.; RL, E. O.; Dos Santos, E. O.; Machado, C. M. D.; Szopa, S.; Zhao, Y.; Alves, E. G.; De Sa, S. S.; Hu, W.; Knipping, E. M.; Shaw, S. L.; Duvoisin Junior, S.; de Souza, R. A. F.; Palm, B. B.; Jimenez, J. L.; Glasius, M.; Goldstein, A. H.; Pye, H. O. T.; Gold, A.; Turpin, B. J.; Vizuete, W.; Martin, S. T.; Thornton, J. A.; Dutcher, C. S.; Ault, A. P.; Surratt, J. D. Increasing Isoprene Epoxydiol-to-Inorganic Sulfate Aerosol Ratio Results in Extensive Conversion of Inorganic Sulfate to Organosulfur Forms: Implications for Aerosol Physicochemical Properties. *Environ. Sci. Technol.* **2019**, *53*, 8682−8694.
(29) Pye, H. O. T.; Nenes, A.; Alexander, B.; Ault, A. P.; Barth, M. C.; Clegg, S. L.; Collett, J. L., Jr.; Fahey, K. M.; Hennigan, C. J.; Herrmann, H.; Kanakidou, M.; Kelly, J. T.; Ku, I. T.; McNeill, V. F.; Riemer, N.; Schaefer, T.; Shi, G.; Tilgner, A.; Walker, J. T.; Wang, T.; Weber, R.; Xing, J.; Zaveri, R. A.; Zuend, A. The acidity of atmospheric particles and clouds. *Atmos. Chem. Phys.* **2020**, *20*, 4809−4888.
(30) Bertram, T. H.; Cochran, R. E.; Grassian, V. H.; Stone, E. A. Sea spray aerosol chemical composition: elemental and molecular mimics for laboratory studies of heterogeneous and multiphase reactions. *Chem. Soc. Rev.* **2018**, *47*, 2374−2400.
(31) De Haan, D. O.; Brauers, T.; Oum, K.; Stutz, J.; Nordmeyer, T.; Finlayson-Pitts, B. J. Heterogeneous chemistry in the troposphere: Experimental approaches and applications to the chemistry of sea salt particles. *Int. Rev. Phys. Chem.* **1999**, *18*, 343−385.
(32) Alexander, B.Sulfate formation in sea-salt aerosols: Constraints from oxygen isotopes. *J. Geophys. Res.: Atmos.***2005**, *110* (), DOI: 10.1029/2004JD005659.
(33) McInnes, L. M.; Covert, D. S.; Quinn, P. K.; Germani, M. S. Measurements of chloride depletion and sulfur enrichment in individual sea-salt particles collected from the remote marine boundary layer. *J. Geophys. Res.: Atmos.* **1994**, *99*, 8257.
(34) Chi, J. W.; Li, W. J.; Zhang, D. Z.; Zhang, J. C.; Lin, Y. T.; Shen, X. J.; Sun, J. Y.; Chen, J. M.; Zhang, X. Y.; Zhang, Y. M.; Wang, W. X. Sea salt aerosols as a reactive surface for inorganic and organic acidic gases in the Arctic troposphere. *Atmos. Chem. Phys.* **2015**, *15*, 11341−11353.
(35) Gard, E. E.; Kleeman, M. J.; Gross, D. S.; Hughes, L. S.; Allen, J. O.; Morrical, B. D.; Fergenson, D. P.; Dienes, T.; Galli, M. E.; Johnson, R. J.; Cass, G. R.; Prather, K. A. Direct Observation of Heterogeneous Chemistry in the Atmosphere. *Science* **1998**, *279*, 1184−1187.
(36) Kirpes, R. M.; Bondy, A. L.; Bonanno, D.; Moffet, R. C.; Wang, B.; Laskin, A.; Ault, A. P.; Pratt, K. A. Secondary sulfate is internally mixed with sea spray aerosol and organic aerosol in the winter Arctic. *Atmos. Chem. Phys.* **2018**, *18*, 3937−3949.

https://doi.org/10.1021/acsearthspacechem.2c00156
ACS Earth Space Chem. XXXX, XXX, XXX−XXX

(37) Bauer, S. E.; Ault, A.; Prather, K. A. Evaluation of aerosol mixing state classes in the GISS modelE-MATRIX climate model using single-particle mass spectrometry measurements. *J. Geophys. Res.: Atmos.* **2013**, *118*, 9834−9844.
(38) Hatch, L. E.; Creamean, J. M.; Ault, A. P.; Surratt, J. D.; Chan, M. N.; Seinfeld, J. H.; Edgerton, E. S.; Su, Y.; Prather, K. A. Measurements of isoprene-derived organosulfates in ambient aerosols by aerosol time-of-flight mass spectrometry-part 2: temporal variability and formation mechanisms. *Environ. Sci. Technol.* **2011**, *45*, 8648−8655.
(39) Bondy, A. L.; Wang, B.; Laskin, A.; Craig, R. L.; Nhliziyo, M. V.; Bertman, S. B.; Pratt, K. A.; Shepson, P. B.; Ault, A. P. Inland Sea Spray Aerosol Transport and Incomplete Chloride Depletion: Varying Degrees of Reactive Processing Observed during SOAS. *Environ. Sci. Technol.* **2017**, *51*, 9533−9542.
(40) Angle, K. J.; Crocker, D. R.; Simpson, R. M. C.; Mayer, K. J.; Garofalo, L. A.; Moore, A. N.; Mora Garcia, S. L.; Or, V. W.; Srinivasan, S.; Farhan, M.; Sauer, J. S.; Lee, C.; Pothier, M. A.; Farmer, D. K.; Martz, T. R.; Bertram, T. H.; Cappa, C. D.; Prather, K. A.; Grassian, V. H. Acidity across the interface from the ocean surface to sea spray aerosol. *Proc. Natl. Acad. Sci. U. S. A.* **2021**, *118*, No. e2018397118.
(41) Keene, W. C.; Pszenny, A. A. P.; Maben, J. R.; Stevenson, E.; Wall, A. Closure evaluation of size-resolved aerosol pH in the New England coastal atmosphere during summer. *J. Geophys. Res.: Atmos.* **2004**, *109*, 1−16.
(42) Nguyen, T. B.; Coggon, M. M.; Bates, K. H.; Zhang, X.; Schwantes, R. H.; Schilling, K. A.; Loza, C. L.; Flagan, R. C.; Wennberg, P. O.; Seinfeld, J. H. Organic aerosol formation from the reactive uptake of isoprene epoxydiols (IEPOX) onto non-acidified inorganic seeds. *Atmos. Chem. Phys.* **2014**, *14*, 3497−3510.
(43) Lin, Y.-H.; Budisulistiorini, S. H.; Chu, K.; Siejack, R. A.; Zhang, H.; Riva, M.; Zhang, Z.; Gold, A.; Kautzman, K. E.; Surratt, J. D. Light-Absorbing Oligomer Formation in Secondary Organic Aerosol from Reactive Uptake of Isoprene Epoxydiols. *Environ. Sci. Technol.* **2014**, *48*, 12012−12021.
(44) Bates, K. H.; Crounse, J. D.; St. Clair, J. M.; Bennett, N. B.; Nguyen, T. B.; Seinfeld, J. H.; Stoltz, B. M.; Wennberg, P. O. Gas Phase Production and Loss of Isoprene Epoxydiols. *The Journal of Physical Chemistry A* **2014**, *118*, 1237−1246.
(45) Hettiyadura, A. P. S.; Al-Naiema, I. M.; Hughes, D. D.; Fang, T.; Stone, E. A. Organosulfates in Atlanta, Georgia: anthropogenic influences on biogenic secondary organic aerosol formation. *Atmos. Chem. Phys.* **2019**, *19*, 3191−3206.
(46) Glasius, M.; Bering, M. S.; Yee, L. D.; de Sá, S. S.; Isaacman-VanWertz, G.; Wernis, R. A.; Barbosa, H. M. J.; Alexander, M. L.; Palm, B. B.; Hu, W.; Campuzano-Jost, P.; Day, D. A.; Jimenez, J. L.; Shrivastava, M.; Martin, S. T.; Goldstein, A. H. Organosulfates in aerosols downwind of an urban region in central Amazon. *Environ. Sci.: Processes Impacts* **2018**, *20*, 1546−1558.
(47) Zhang, Z.; Lin, Y. H.; Zhang, H.; Surratt, J. D.; Ball, L. M.; Gold, A. Technical Note: Synthesis of isoprene atmospheric oxidation products: isomeric epoxydiols and the rearrangement products cis- and trans-3-methyl-3,4-dihydroxytetrahydrofuran. *Atmos. Chem. Phys.* **2012**, *12*, 8529−8535.
(48) Lin, Y. H.; Zhang, Z. F.; Docherty, K. S.; Zhang, H. F.; Budisulistiorini, S. H.; Rubitschun, C. L.; Shaw, S. L.; Knipping, E. M.; Edgerton, E. S.; Kleindienst, T. E.; Gold, A.; Surratt, J. D. Isoprene Epoxydiols as Precursors to Secondary Organic Aerosol Formation: Acid-Catalyzed Reactive Uptake Studies with Authentic Compounds. *Environ. Sci. Technol.* **2012**, *46*, 250−258.
(49) Craig, R. L.; Peterson, P. K.; Nandy, L.; Lei, Z.; Hossain, M. A.; Camarena, S.; Dodson, R. A.; Cook, R. D.; Dutcher, C. S.; Ault, A. P. Direct Determination of Aerosol pH: Size-Resolved Measurements of Submicrometer and Supermicrometer Aqueous Particles. *Anal. Chem.* **2018**, *90*, 11232−11239.
(50) Lei, Z.; Olson, N. E.; Zhang, Y.; Chen, Y.; Lambe, A. T.; Zhang, J.; White, N. J.; Atkin, J. M.; Banaszak Holl, M. M.; Zhang, Z.; Gold, A.; Surratt, J. D.; Ault, A. P. Morphology and Viscosity Changes after Reactive Uptake of Isoprene Epoxydiols in Submicrometer Phase Separated Particles with Secondary Organic Aerosol Formed from Different Volatile Organic Compounds. *ACS Earth Space Chem.* **2022**, *6*, 871−882.
(51) Pratt, K. A.; Mayer, J. E.; Holecek, J. C.; Moffet, R. C.; Sanchez, R. O.; Rebotier, T. P.; Furutani, H.; Gonin, M.; Fuhrer, K.; Su, Y.; Guazzotti, S.; Prather, K. A. Development and Characterization of an Aircraft Aerosol Time-of-Flight Mass Spectrometer. *Anal. Chem.* **2009**, *81*, 1792−1800.
(52) Budisulistiorini, S. H.; Canagaratna, M. R.; Croteau, P. L.; Marth, W. J.; Baumann, K.; Edgerton, E. S.; Shaw, S. L.; Knipping, E. M.; Worsnop, D. R.; Jayne, J. T.; Gold, A.; Surratt, J. D. Real-Time Continuous Characterization of Secondary Organic Aerosol Derived from Isoprene Epoxydiols in Downtown Atlanta, Georgia, Using the Aerodyne Aerosol Chemical Speciation Monitor. *Environ. Sci. Technol.* **2013**, *47*, 5686−5694.
(53) Ng, N. L.; Herndon, S. C.; Trimborn, A.; Canagaratna, M. R.; Croteau, P. L.; Onasch, T. B.; Sueper, D.; Worsnop, D. R.; Zhang, Q.; Sun, Y. L.; Jayne, J. T. An Aerosol Chemical Speciation Monitor (ACSM) for Routine Monitoring of the Composition and Mass Concentrations of Ambient Aerosol. *Aerosol Sci. Technol.* **2011**, *45*, 780−794.
(54) Budisulistiorini, S. H.; Li, X.; Bairai, S. T.; Renfro, J.; Liu, Y.; Liu, Y. J.; McKinney, K. A.; Martin, S. T.; McNeill, V. F.; Pye, H. O. T.; Nenes, A.; Neff, M. E.; Stone, E. A.; Mueller, S.; Knote, C.; Shaw, S. L.; Zhang, Z.; Gold, A.; Surratt, J. D. Examining the effects of anthropogenic emissions on isoprene-derived secondary organic aerosol formation during the 2013 Southern Oxidant and Aerosol Study (SOAS) at the Look Rock, Tennessee ground site. *Atmos. Chem. Phys.* **2015**, *15*, 8871−8888.
(55) Laskina, O.; Morris, H. S.; Grandquist, J. R.; Estillore, A. D.; Stone, E. A.; Grassian, V. H.; Tivanski, A. V. Substrate-Deposited Sea Spray Aerosol Particles: Influence of Analytical Method, Substrate, and Storage Conditions on Particle Size, Phase, and Morphology. *Environ. Sci. Technol.* **2015**, *49*, 13447−13453.
(56) Chen, Q.; Edebeli, J.; McNamara, S. M.; Kulju, K. D.; May, N. W.; Bertman, S. B.; Thanekar, S.; Fuentes, J. D.; Pratt, K. A. HONO, Particulate Nitrite, and Snow Nitrite at a Midlatitude Urban Site during Wintertime. *ACS Earth Space Chem.* **2019**, *3*, 811−822.
(57) Kulju, K. D.; McNamara, S. M.; Chen, Q.; Kenagy, H. S.; Edebeli, J.; Fuentes, J. D.; Bertman, S. B.; Pratt, K. A. Urban inland wintertime N2O5 and ClNO2 influenced by snow-covered ground, air turbulence, and precipitation. *Atmos. Chem. Phys.* **2022**, *22*, 2553−2568.
(58) Chen, Y.; Zhang, Y.; Lambe, A. T.; Xu, R.; Lei, Z.; Olson, N. E.; Zhang, Z.; Szalkowski, T.; Cui, T.; Vizuete, W.; Gold, A.; Turpin, B. J.; Ault, A. P.; Chan, M. N.; Surratt, J. D. Heterogeneous Hydroxyl Radical Oxidation of Isoprene-Epoxydiol-Derived Methyltetrol Sulfates: Plausible Formation Mechanisms of Previously Unexplained Organosulfates in Ambient Fine Aerosols. *Environ. Sci. Technol. Lett.* **2020**, *7*, 460−468.
(59) Cui, T.; Zeng, Z.; Dos Santos, E. O.; Zhang, Z.; Chen, Y.; Zhang, Y.; Rose, C. A.; Budisulistiorini, S. H.; Collins, L. B.; Bodnar, W. M.; de Souza, R. A. F.; Martin, S. T.; Machado, C. M. D.; Turpin, B. J.; Gold, A.; Ault, A. P.; Surratt, J. D. Development of a hydrophilic interaction liquid chromatography (HILIC) method for the chemical characterization of water-soluble isoprene epoxydiol (IEPOX)-derived secondary organic aerosol. *Environ. Sci.: Processes Impacts* **2018**, *20*, 1524−1536.
(60) Hughes, D. D.; Christiansen, M. B.; Milani, A.; Vermeuel, M. P.; Novak, G. A.; Alwe, H. D.; Dickens, A. F.; Pierce, R. B.; Millet, D. B.; Bertram, T. H.; Stanier, C. O.; Stone, E. A. PM2.5 chemistry, organosulfates, and secondary organic aerosol during the 2017 Lake Michigan Ozone Study. *Atmos. Environ.* **2021**, *244*, No. 117939.
(61) Hughes, D. D.; Stone, E. A. Organosulfates in the Midwestern United States: abundance, composition and stability. *Environ. Chem.* **2019**, *16*, 321−322.
(62) Hatch, L. E.; Creamean, J. M.; Ault, A. P.; Surratt, J. D.; Chan, M. N.; Seinfeld, J. H.; Edgerton, E. S.; Su, Y.; Prather, K. A.

Measurements of isoprene-derived organosulfates in ambient aerosols by aerosol time-of-flight mass spectrometry - part 1: single particle atmospheric observations in Atlanta. *Environ. Sci. Technol.* **2011**, *45*, 5105−5111.
(63) Irish, D. E.; Chen, H. Raman spectral study of bisulfate-sulfate systems. II. Constitution, equilibriums, and ultrafast proton transfer in sulfuric acid. *J. Phys. Chem.* **1971**, *75*, 2672−2681.
(64) Ault, A. P.; Zhao, D.; Ebben, C. J.; Tauber, M. J.; Geiger, F. M.; Prather, K. A.; Grassian, V. H. Raman microspectroscopy and vibrational sum frequency generation spectroscopy as probes of the bulk and surface compositions of size-resolved sea spray aerosol particles. *Phys. Chem. Chem. Phys.* **2013**, *15*, 6206.
(65) Bondy, A. L.; Craig, R. L.; Zhang, Z.; Gold, A.; Surratt, J. D.; Ault, A. P. Isoprene-Derived Organosulfates: Vibrational Mode Analysis by Raman Spectroscopy, Acidity-Dependent Spectral Modes, and Observation in Individual Atmospheric Particles. *J. Phys. Chem. A* **2018**, *122*, 303−315.
(66) Hirakawa, A. Y.; Nishimura, Y.; Matsumoto, T.; Nakanishi, M.; Tsuboi, M. Characterization of a Few Raman Lines of Tryptophan. *J. Raman Spectrosc.* **1978**, *7*, 282−287.
(67) Baran, J.; Barnes, A. J.; Ratajczak, H. Polarized infrared and Raman spectra of diglycine nitrate single crystal. *Spectrochim. Acta* **1995**, *51A*, 197−214.
(68) Schulz, H.; Baranska, M. Identification and quantification of valuable plant substances by IR and Raman spectroscopy. *Vib. Spectrosc.* **2007**, *43*, 13−25.
(69) Larkin, P. J., *Infrared and Raman Spectroscopy*. Elsevier Inc.: 2011.
(70) Fankhauser, A. M.; Lei, Z.; Daley, K. R.; Xiao, Y.; Zhang, Z.; Gold, A.; Ault, B. S.; Surratt, J. D.; Ault, A. P. Acidity-Dependent Atmospheric Organosulfate Structures and Spectra: Exploration of Protonation State Effects via Raman and Infrared Spectroscopies Combined with Density Functional Theory. *J. Phys. Chem. A* **2022**, *126*, 5974−5984.
(71) Lei, Z.; Chen, Y.; Zhang, Y.; Cooke, M. E.; Ledsky, I. R.; Armstrong, N. C.; Olson, N. E.; Zhang, Z.; Gold, A.; Surratt, J. D.; Ault, A. P. Initial pH Governs Secondary Organic Aerosol Phase State and Morphology after Uptake of Isoprene Epoxydiols (IEPOX). *Environ. Sci. Technol.* **2022**, *56*, 10596−10607.
(72) Zhang, Y.; Chen, Y.; Lambe, A. T.; Olson, N. E.; Lei, Z.; Craig, R. L.; Zhang, Z.; Gold, A.; Onasch, T. B.; Jayne, J. T.; Worsnop, D. R.; Gaston, C. J.; Thornton, J. A.; Vizuete, W.; Ault, A. P.; Surratt, J. D. Effect of the Aerosol-Phase State on Secondary Organic Aerosol Formation from the Reactive Uptake of Isoprene-Derived Epoxydiols (IEPOX). *Env. Sci. Tech. Lett.* **2018**, *5*, 167−174.
(73) Olson, N. E.; Lei, Z.; Craig, R. L.; Zhang, Y.; Chen, Y.; Lambe, A. T.; Zhang, Z.; Gold, A.; Surratt, J. D.; Ault, A. P. Reactive Uptake of Isoprene Epoxydiols Increases the Viscosity of the Core of Phase-Separated Aerosol Particles. *ACS Earth Space Chem.* **2019**, *3*, 1402−1414.
(74) Angle, K.; Grassian, V.; Ault, A. The rapid acidification of sea spray aerosols. *Phys. Today* **2022**, 58−58.
(75) May, N. W.; Gunsch, M. J.; Olson, N. E.; Bondy, A. L.; Kirpes, R. M.; Bertman, S. B.; China, S.; Laskin, A.; Hopke, P. K.; Ault, A. P.; Pratt, K. A. Unexpected Contributions of Sea Spray and Lake Spray Aerosol to Inland Particulate Matter. *Environ. Sci. Technol. Lett.* **2018**, *5*, 405−412.

https://doi.org/10.1021/acsearthspacechem.2c00156
ACS Earth Space Chem. XXXX, XXX, XXX−XXX